**Proceedings of the ASME 2017 International Design Engineering Technical Conferences and
Computers and Information in Engineering Conference
IDETC/CIE 2017
August 6-9, 2017, Cleveland, Ohio, USA**

DETC2017-68246

QUANTIFYING ALMOND WATER STRESS USING UNMANNED AERIAL VEHICLES (UAVS): CORRELATION OF STEM WATER POTENTIAL AND HIGHER ORDER MOMENTS OF NON-NORMALIZED CANOPY DISTRIBUTION

Tiebiao Zhao
Mechatronics, Embedded Systems and Automation Lab
University of California, Merced
Merced, California 95343
Email: tzhao3@ucmerced.edu

YangQuan Chen[*]
Mechatronics, Embedded Systems and Automation Lab
University of California
Merced, California, 95343
ychen53@ucmerced.edu

Andrew Ray
University of California,Cooperative Extension
Merced, California, 95341-6445
Email: alray@ucanr.edu

David Doll
University of California,Cooperative Extension
Merced, California, 95341-6445
Email: dadoll@ucanr.edu

ABSTRACT

Optimization of water use relies on accurate measurement of water status of crops. Stem water potential (SWP) has become one of the most popular methods to monitor the water status of almond trees. However, it needs to take twice visit and at least thirty minutes to obtain one measurement, which makes it very difficult to understand the water status information in the orchard level. Unmanned aerial vehicle (UAV) based remote sensing promises to deliver reliable and precise field-scale information more efficiently by providing multispectral higher-resolution images with much lower cost and higher flexibility. This paper aims to extract almond water status from UAV-based multispectral images via building the correlation between SWP and vegetation indices. Different from the traditional method that focuses on normalized difference vegetation index (NDVI) means, higher-order moments of non-normalized canopy distribution descriptors were discussed to model SWP measurements. Results showed that the proposed methods performed better than traditional NDVI mean.

INTRODUCTION

By value, almonds are the top one export agriculture products in California, where over 82 percent of global almonds are produced [1]. There has been steady growth in the amount of acreage dedicated to almonds production with 900,000 acres planted in 2016, up from 442,000 acres in 1997 [2]. Just in the past year, almost 108,000 acres of almonds were planted (USDA, 2016). Almonds are water-intensive crop, using 9.5 percent of the states' agricultural water. However, California has been experiencing severe drought since winter 2011. Back to November [3], 2016, 75 percent of California was under drought, along with 43 percent of California enduring extreme to exceptional drought. Driven by the high value of the crop community, the increased growth and serious water scarcity in the state, it is imperative to develop efficient irrigation strategies for almond production.

Optimization of the irrigation lies on accurate measurement of the water status in the plants. Instead of soil moisture, telling the information in the limited region, and evapotranspiration, indicating water loss from weather changes, stem water potential (SWP) measures the water status of plants directly. It has been

---

[*]Corresponding author

Copyright © 2017 ASME
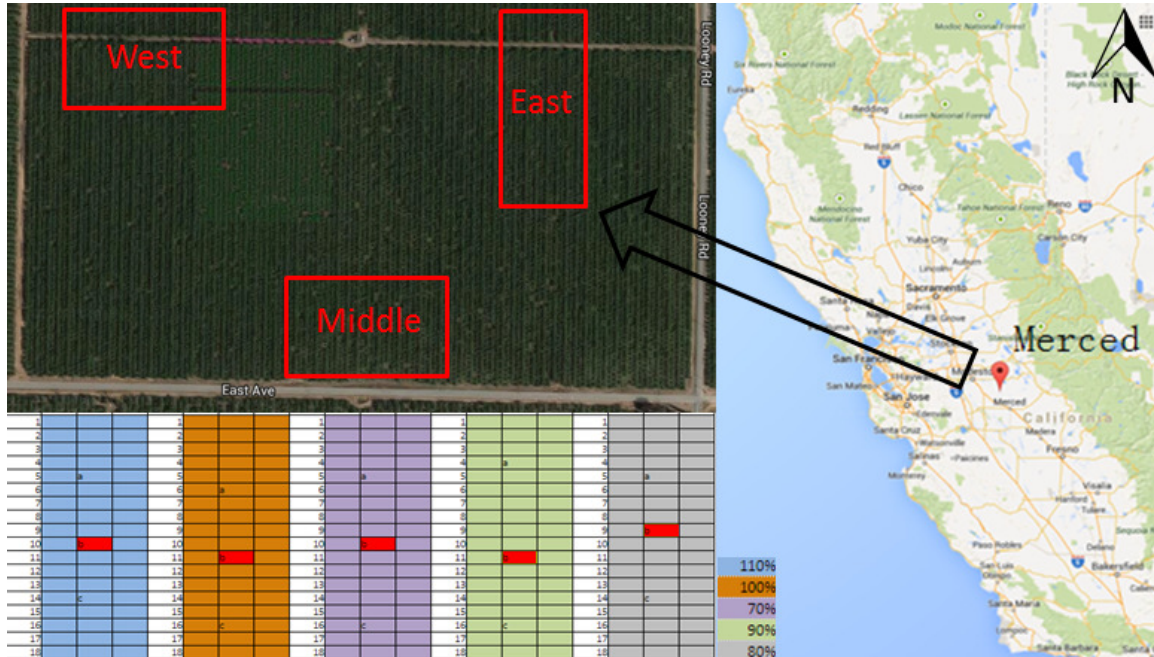
FIGURE 1. OVERVIEW OF TESTFIELD, INCLUDING THREE TEST BLOCKS IN THE ORCHARD, EACH COMPOSED OF FIVE PLOTS TREATED WITH 70%, 80%,90%,100%,110% of CROP EVAPTRANSPIRATION.

proved to be useful in many fruit tree species and able to indicate short-term and mid-term plant response to stress [4]. Considering at least ten minutes after the sample leaf is covered [5] and twice visit, it is a big challenge to conduct measurements frequently, especially in the large orchard. With the fast development of multispectral cameras and UAV platforms, it is promising to conduct the real-time crop monitoring in a large scale with sufficient accuracy.

Quite a few studies have been conducted on the correlation between SWP and vegetation indices in different species of crops using UAVs based remote sensing. Crop water stress index (CWSI) showed good correlation with SWP in peach trees [6], pistachio trees [7] and almond trees [8]. PRI was correlated well with SWP in olive trees [9] and significant correlation was found between PRI and CWSI in vineyards [10]. NDVI was correlated well with SWP in mandarin citrus trees [11]. Non-normalized NDVI was shown a good correlation with SWP in almond trees [12]. Although the image spatial resolutions and camera band configurations in these studies were different, all these vegetation indices were obtained by averaging the pixel values in the scales of canopy or blocks.

The averages of vegetation indices such as NDVI, were similar under different image resolutions, whether they were obtained from satellites, UAVs, ground spectrometers or hand-hold scanners [13, 14]. This indicates that higher resolution images will not contribute extra accuracy in the final measurement besides fine resolution if just the statistic average is applied. It

was shown that the temperature distribution within individual crowns indicated water stress [8, 15], where canopy temperature distributions of stressed trees showed a positive skewness. Histogram shapes of NDVI, the green normalized difference vegetation Index (GNDVI), and the soil adjusted vegetation index (SAVI) were also used to compare stress levels of different regions [16].

Inspired by these works we are interested in whether we could monitor water status of almond trees by quantifying the histogram shapes of non-normalized canopy distribution [12] via higher order moments. Correlations between SWP and average, skewness and kurtosis of canopy distributions are compared using the data collected in growing season 2015.

MATERIALS AND METHODS
Remote sensing platform

The remote sensing platform includes a quadcopter and a near-infrared(NIR) camera, a red-green-blue(RGB) camera (ELPH110HS, Canon, Japan). The quadcopter was built from scratch using Quadkit (3DRobotics, Berkeley, USA), as shown in Fig. 2. The model aircrast comprises four sets of electric speed controllers (ESCs), brushless motors and plastic propellers, controlled by the ardupilot, mounted on the fiberglass frame with four aluminum arms. Two blue arms indicate forward and two black arms tell backwards.

The NIR camera was modified from a regular Commercial-

Copyright © 2017 ASME

FIGURE 2. THE UAV-BASED REMOTE SENSING PLATFORM INCLUDING A QUADCOPTER, A NIR CAMERA AND A RGB CAMERA, CREDITS TO LARRY BURROW.

off-the-shelf (COTS) RGB camera (ELPH110HS, Canon, Japan) by LDP LLC, USA. The peaks of its blue, green and NIR bands are located in 450nm, 520nm, 720nm. Both RGB and NIR cameras have a resolution 4608×3459, with a radiometric resolution of 24 bit.The camera supported Cannon hack development kit (CHDK), which makes it programmable to trigger cameras via the autopilot. Most importantly, it synchronizes the images with their GPS and IMU information during flights.

Study areas

The study was carried out in a commercial almond orchard located in Merced County, CA, USA(37.493498°N, -120.634914°W). Three varieties Nonpareil, Carmel, and Monterey were planted on Lovell peach rootstocks 16 years ago at a spacing of 5.5 m×6.1 m. The soil of the site is of Rocklin and Greenfield sandy loam. The climate is Mediterranean, characterized by wet, cool, rainy winters and hot, dry summers. The averave anual extreme temperature is between 25°F and 30°F. Three blocks were chosen for the study. Each block comprised five different plots, where five irrigation levels are run, one per plot from 70% to 110% of crop evaptranspiration (ET_c) with increment by 10%. Each plot includes three rows of trees with 18 trees per row, as shown in Fig. 1. The water is delivered accordingly by tuning microsprinklers(Supernet, Netafim).

Crop evapotranspiration was calculated according to Food and Agriculture Orgination (FAO) method [17].

$$ET_c = K_c * ET_o \qquad (1)$$

where ETo is the evapotranspiration rate of a reference surface

under optimum treatment and certain climatic conditions, and crop coefficient K_c is defined as the ratio ETc/ETo. K_c utilized in this study was developed in California [18].

Field measurements

Concomitant to each flight and multispectral image acquisition, stem water potential ψ_s were measured with the aim of comparing image-based results with a ground-truthed indicator. The ψ_s of fifteen trees were measured within a block, three trees per irrigation level in the center of the plot, as marked in Fig. 1. One block was measured each week and three blocks were measured in truns. A lower shaded bagged leave was taken from each sample tree and was measured with a pressure chamber (PMS Instrument Model 600, Oregon, USA) following the recommendations [5].

Airborne imagery

The airborne compaign were conducted at 60 meters above the ground and the spatial resolution was 1.87 cm/pix. The cameras were triggered at a distance of 16 m to obtain the overlap upto 75% in order to stitch images using the software PhotoScan (Agisoft,Russia). The images of white panels and dark panels were taken right before flight missions serving as reflectance references. The digital number (DN) value of raw image is converted to reflectance with an empirical method [19] as shown in Eqn.2. The DN of dark panels (DN_D) and white panels (DN_W) are determined by the point located in the central part of its histogram. NDVI is calculated according to Eqn.3, where the reflectance in the red band (ρ_R) is replaced with that of the blue band (ρ_B). It is reasonable because the distance between objects and cameras is 60 meters and atmosphere scattering and absorption would not have a significant effect in the blue band. Most importantly, this saves effort to register the images between bands and decreases error from low regeneration accuracy.

To minimize the influence of bidirectional reflectance distribution function (BRDF) effects [20], only the canopy images collected with nadir view angles were used. Then the canopy image of each sample tree was separated from soil manually and the pixels within the canopy were further analyzed.

$$\rho_\lambda = \frac{DN - DN_D}{DN_W - DN_D} \qquad (2)$$

$$NDVI = \frac{\rho_{NIR} - \rho_B}{\rho_{NIR} + \rho_B}. \qquad (3)$$

Copyright © 2017 ASME
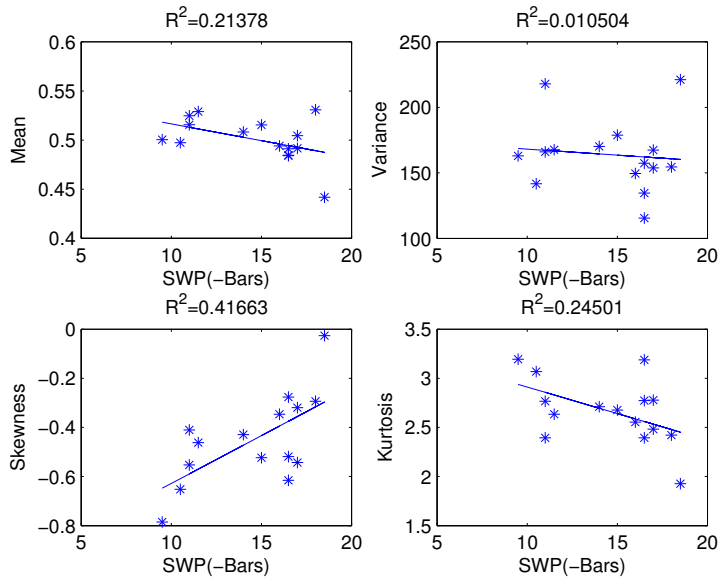
FIGURE 3. CORRELATION BETWEEN SWP AND MEAN, VARIANCE, SKEWNESS AND KURTOSIS USING DATA COLLECTED IN THE MIDDLE BLOCK ON JUNE 18TH,2015.
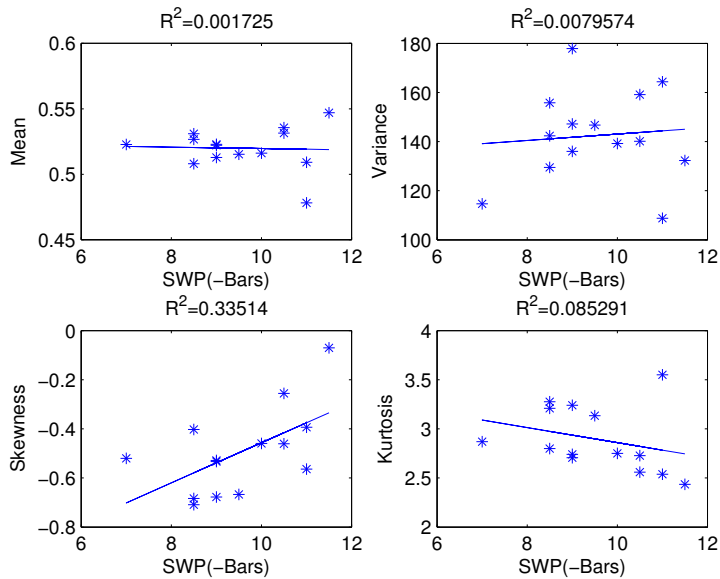
FIGURE 4. CORRELATION BETWEEN SWP AND MEAN, VARIANCE, SKEWNESS AND KURTOSIS USING DATA COLLECTED IN THE EAST BLOCK ON JULY 16TH, 2015.

RESULTS AND DISCUSSIONS

Non-normalized NDVI index was compared with traditional NDVI in [12]. In the study, we are interested in how the higher order moments of canopy distributions are related to SWP mea-surements. After canopy images seperated from soil, the DN value difference between the NIR band and blue band of every pixel within canopies was calculated, Then for each sample tree, its canopy distribution was described using the histogram of DN

4

Copyright © 2017 ASME
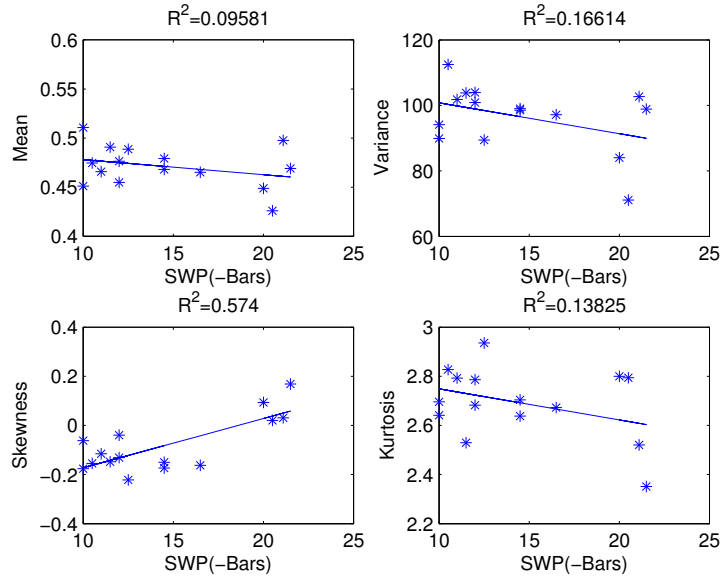
FIGURE 5. CORRELATION BETWEEN SWP AND MEAN, VARIANCE, SKEWNESS AND KURTOSIS USING DATA COLLECTED IN THE MIDDLE BLOCK ON AUGUST 20TH, 2015.

TABLE 1. MODELING PERFORMANCE PARAMETERS BETWEEN SKEWNESS AND SWP WITHIN THREE DIFFERENT MONTHS

Parameters	06-18-2015	07-16-2015	08-20-2015
R^2	0.4166	0.3351	0.574
pValue (Intercept)	0.00013054	0.0017892	0.00018639
pValue (Skewness)	0.0093539	0.030068	0.0010684

value difference of all the pixels within the canopy, where the range of DN value difference is 0 to 255 and the number of bins is 255. Variance, skewness and kurtosis of canopy distributions were calculated based on the its histogram of DN value difference. Traditional canopy NDVI average was also calculated as a reference. Correlations analysis between these four vegetation indices and SWP measurements of sample trees on June 18th, July 16th and August 20th, 2015 were conducted to compare their performance. Statistic analysis was carried out in Matlab2013b (Mathworks, Massachusetts, United States).

Figures 3 to 5 show scatter plots and fitted line between vegetation indices and SWP measurements collected in three different months. In each figure, x axis stands for SWP and y axes stand for canopy NDVI means, variances of canopy DN difference distribution, skewness of canopy DN difference distribution, kurtosis of canopy DN difference distribution in order. R^2 is labeled on top of each subfigure. It is demonstrated that skew-

ness performs the best among all these features. This can be explained in the way that the larger the skewness, the more pixels in the left part of its histogram, where the DN difference is smaller and the region is under higher stress. R^2, pValue of intercept and skewness on three months are listed in Tab.1, showing the correlations are significant ($p<0.05$).

CONCLUSION

The development of UAVs and payloads makes it easier to collect images with higher spatial resolution than those of satellites. With this bigger data, it is possible to monitor crops with not only higher spatial resolution, but also higher accuracy. Contrast to traditional vegetation indices such as NDVI average [21, 22], new types of vegetation indices are necessary to extract more information from images. The paper continues the research of non-normalized NDVI [12] and discusses the relationship between higher order moments of canopy distributions and SWP. Statistical analysis shows skewness has the best linear correlation with SWP and it is aligned with the findings in [8,16].

5

Copyright © 2017 ASME

and Jacob Clark for contributions in conducting flight missions in the 2015 growing season.

REFERENCES

[1] California Department of Food and Agriculture. 2015 Crop Year Report. On the WWW. URL http://www.cdfa.ca.gov/statistics.

[2] Dan Bacher, 2016. 77,000 acres of thirsty new california almond orchards planted over past year. On the WWW. URL http://www.dailykos.com.

[3] United States Drought Monitor, 2016. On the WWW. URL http://droughtmonitor.unl.edu/.

[4] Shackel, K. A., 1995. "Plant water status as an index of irrigation needs in deciduous fruit trees". *HortScience, 30*(4), pp. 905–905.

[5] Fulton, A., Grant, J., Buchner, R., and Connell, J., 2014. "Using the pressure chamber for irrigation management in walnut, almond, and prune". *Oakland: University of California Division of Agriculture and Natural Resources Publication, 8503*.

[6] Bellvert, J., Marsal, J., Girona, J., Gonzalez-Dugo, V., Fereres, E., Ustin, S. L., and Zarco-Tejada, P. J., 2016. "Airborne thermal imagery to detect the seasonal evolution of crop water status in peach, nectarine and saturn peach orchards". *Remote Sensing, 8*(1), p. 39.

[7] Gonzalez-Dugo, V., Goldhamer, D., Zarco-Tejada, P., and Fereres, E., 2015. "Improving the precision of irrigation in a pistachio farm using an unmanned airborne thermal system". *Irrigation Science, 33*(1), pp. 43–52.

[8] Gonzalez-Dugo, V., Zarco-Tejada, P., Berni, J. A., Suárez, L., Goldhamer, D., and Fereres, E., 2012. "Almond tree canopy temperature reveals intra-crown variability that is water stress-dependent". *Agricultural and Forest Meteorology, 154*, pp. 156–165.

[9] Suárez, L., Zarco-Tejada, P., González-Dugo, V., Berni, J., and Fereres, E., 2008. "Detecting water stress in orchard crops using pri from airborne imagery". In 6th EARSeL SIG IS workshop imaging Spectroscopy: Innovative tool for scientific and commercial environmental applications, March 16–19, 2009, Tel-Aviv, Israel.

[10] Zarco-Tejada, P. J., González-Dugo, V., Williams, L., Suárez, L., Berni, J. A., Goldhamer, D., and Fereres, E., 2013. "A pri-based water stress index combining structural and chlorophyll effects: Assessment using diurnal narrow-band airborne imagery and the cwsi thermal index". *Remote sensing of environment, 138*, pp. 38–50.

[11] Romero-Trigueros, C., Nortes, P. A., Alarcón, J. J., Hunink, J. E., Parra, M., Contreras, S., Droogers, P., and Nicolás, E., 2016. "Effects of saline reclaimed waters and deficit irrigation on citrus physiology assessed by uav remote sensing". *Agricultural Water Management*.

[12] Zhao, T., Stark, B., Chen, Y., Ray, A., and Doll, D., 2016. "More reliable crop water stress quantification using small unmanned aerial systems (suas)". *IFAC-PapersOnLine, 49*(16), pp. 409–414.

[13] Matese, A., Toscano, P., Di Gennaro, S. F., Genesio, L., Vaccari, F. P., Primicerio, J., Belli, C., Zaldei, A., Bianconi, R., and Gioli, B., 2015. "Intercomparison of uav, aircraft and satellite remote sensing platforms for precision viticulture". *Remote Sensing, 7*(3), pp. 2971–2990.

[14] Zheng, H., Zhou, X., Cheng, T., Yao, X., Tian, Y., Cao, W., and Zhu, Y., 2016. "Evaluation of a uav-based hyperspectral frame camera for monitoring the leaf nitrogen concentration in rice". In Geoscience and Remote Sensing Symposium (IGARSS), 2016 IEEE International, IEEE, pp. 7350–7353.

[15] Agam, N., Segal, E., Peeters, A., Levi, A., Dag, A., Yermiyahu, U., and Ben-Gal, A., 2014. "Spatial distribution of water status in irrigated olive orchards by thermal imaging". *Precision agriculture, 15*(3), pp. 346–359.

[16] Candiago, S., Remondino, F., De Giglio, M., Dubbini, M., and Gattelli, M., 2015. "Evaluating multispectral images and vegetation indices for precision farming applications from uav images". *Remote Sensing, 7*(4), pp. 4026–4047.

[17] Allen, R. G., Pereira, L. S., Raes, D., Smith, M., et al., 1998. "Crop evapotranspiration-guidelines for computing crop water requirements-fao irrigation and drainage paper 56". *FAO, Rome, 300*(9), p. D05109.

[18] Doll, D., and Shackel, K., 2016. "Drought management for california almonds". *Crops and Soils, 49*(2), pp. 28–35.

[19] Smith, G. M., and Milton, E. J., 1999. "The use of the empirical line method to calibrate remotely sensed data to reflectance". *International Journal of remote sensing, 20*(13), pp. 2653–2662.

[20] Stark, B., Zhao, T., and Chen, Y., 2016. "An analysis of the effect of the bidirectional reflectance distribution function on remote sensing imagery accuracy from small unmanned aircraft systems". In Unmanned Aircraft Systems (ICUAS), 2016 International Conference on, IEEE, pp. 1342–1350.

[21] Zhao, T., Stark, B., Chen, Y., Ray, A. L., and Doll, D., 2015. "A detailed field study of direct correlations between ground truth crop water stress and normalized difference vegetation index (ndvi) from small unmanned aerial system (suas)". In Unmanned Aircraft Systems (ICUAS), 2015 International Conference on, IEEE, pp. 520–525.

[22] Zhao, T., Stark, B., Chen, Y., Ray, A. L., and Doll, D., 2016. "Challenges in water stress quantification using small unmanned aerial system (suas): Lessons from a growing season of almond". In Unmanned Aircraft Systems (ICUAS), 2016 International Conference on, IEEE, pp. 1366–1370.